第16卷第11期
2026年11月

中国无机分析化学
Chinese Journal of Inorganic Analytical Chemistry

Vol. 16, No. 11
2125～2134

doi: 10. 20236/j. CJIAC. 2026. 11. 016

陈曦，李源珂，岳虹丞，等. 远程激光诱导击穿光谱(LIBS)技术定量分析合金钢中铬和锰[J]. 中国无机分析化学，2026，16(11)：2125-2134.

Chen Xi, Li Yuanke, Yue Hongcheng, et al. Quantitative Analysis of Chromium and Manganese in Alloy Steel by Remote Laser-induced Breakdown Spectroscopy (LIBS) [J]. Chinese Journal of Inorganic Analytical Chemistry, 2026, 16(11): 2125-2134.

远程激光诱导击穿光谱(LIBS)技术定量分析合金钢中铬和锰

陈 曦[1,2]　李源珂[3]　岳虹丞[3]　汤 悦[3]　田俊朗[1,2]
牛广辉[4*]　孙 旋[1,2*]　林庆宇[3*]

(1.桂林理工大学 广西高校先进制造与自动化技术重点实验室，广西 桂林 541006；
2.桂林理工大学 机械与控制工程学院，广西 桂林 541004；
3.四川大学 机械工程学院，成都 610064；
4.宝武装备智能科技有限公司 科技创新部(技术(研发)中心)，上海 201900)

摘　要　检测钢铁产品或原料中的化学元素组成是控制产品质量的关键。激光诱导击穿光谱(LIBS)技术具有远距离测试的能力，可在高温、辐射等危险环境实现对生产产品的远程原位定量分析。本研究基于便携远程LIBS仪器，在3 m距离下对12种合金钢标准样品进行光谱采集。在优化激光脉冲的激发累加次数后，利用线性拟合、二次多项式拟合、优化分段点后的分段线性拟合及分段内标线性拟合建立定标曲线，根据最佳拟合度的拟合方式对合金钢中Cr和Mn两种元素进行定量分析。结果显示，Cr和Mn两种元素预测值的相对误差最小值分别为8. 34%和7. 38%，均方根误差最小值分别为1. 09%和0. 049%，相对标准偏差最小值分别为3. 7%和11. 3%，验证了该仪器对钢铁中元素定量的可行性。本研究证实，与目前广泛研究的多变量算法定量相比，利用单变量定标方法，通过优化分析参数及拟合方式进行定量，可为合金钢中元素的工业现场检测提供一种简单可靠的定量方案。

关键词　激光诱导击穿光谱；远程定量分析；合金钢；铬；锰

要点

1) 利用远程LIBS系统对合金钢标准样品中Cr和Mn进行了定量分析。

2) 优化了不同激光激发次数对特征光谱的影响。

3) 研究了四种拟合方式定标曲线的效果并对分段拟合的分段点进行了优化。

中图分类号：O657. 38　　**文献标志码**：A　　**文章编号**：2095-1035(2026)11-2125-10

收稿日期：2026-01-08　　**修回日期**：2026-03-01　　**录用日期**：2026-03-17　　**在线出版日期**：2026-06-17

Received：2026-01-08　　**Revised**：2026-03-01　　**Accepted**：2026-03-17　　**Online published**：2026-06-17

基金项目：广西重点研发计划项目(2024AB09023)

Fund：Supported by the Guangxi Key Research and Development Program Project (2024AB09023)

作者简介：陈曦，女，硕士研究生，主要从事激光光谱方法研究。E-mail：534948177@qq. com

Author：Chen Xi, female, master candidate, mainly engaged in research on laser spectroscopy methods. E-mail：534948177@qq. com

*通信作者：牛广辉，男，博士，主要从事等离子体技术应用与装备研究。E-mail：niuguanghui@baosteel. com

孙旋，男，副教授，主要从事机电控制技术研究。E-mail：sunxuan@glut. edu. cn

林庆宇，男，副研究员，主要从事激光光谱分析仪器研究。E-mail：qylin@scu. edu. cn

*Corresponding author：Niu Guanghui, male, Ph. D., mainly engaged in research on plasma technology applications and equipment. E-mail：niuguanghui@baosteel. com

Sun Xuan, male, associate professor, mainly engaged in research on electromechanical control technology. E-mail：sunxuan@glut. edu. cn

Lin Qingyu, male, associate researcher, mainly engaged in research on laser spectroscopy analysis instruments. E-mail：qylin@scu. edu. cn

©Chinese Journal of Inorganic Analytical Chemistry Editorial Department 2026. This is an open access article under the CC-BY-NC-ND 4.0 License.

钢铁作为现代工业的基石，在国防建设、能源开发、交通运输及装备制造等关键领域广泛应用，对我国经济社会的发展起着重要作用[1]。随着工业生产智能化发展，在生产效率不断提高的同时，对钢铁产品或原料中的化学元素组成进行检测的准确性、快捷性及可靠性要求越来越高[2]。据统计，约40%的钢铁质量问题与钢中元素成分不准确有关，每年经济损失达数十亿元[3]。为控制钢铁产品质量需检测钢铁材料的元素组成。钢材的性能主要由其组成成分决定[4]，Fe、Cr 和 Mn 等元素是钢铁合金的重要组成成分，其中Cr 和 Mn 等元素含量影响钢铁材料性能，如过量的Cr增加材料的脆性及降低材料塑韧性[5]，而高含量的Mn易引发钢材硬脆化问题[6]。因此，对合金钢中Cr和Mn的定量分析十分必要。传统常用的元素分析方法有火花直读发射光谱法(Spark-OES)[7-8]、原子吸收光谱法(AAS)[9-10]、电感耦合等离子体发射光谱法(ICP-OES)[11-12]、X射线荧光光谱法(XRF)[13-14]等。基于AAS和ICP-OES技术的分析方法虽准确度高，但需要对合金样本进行耗时的化学消解预处理[15-16]，而XRF 和 Spark-OES技术仅需对合金样品进行简单前处理，具备直接分析样品的能力[17-18]，但分析速度仍难以满足冶金工业现场大批量样本的快速实时分析新需求。

激光诱导击穿光谱技术(LIBS)作为一种原子发射光谱分析技术，通过将高能脉冲激光聚焦至样品表面产生等离子体，并基于等离子体光谱实现元素定性及定量分析。该技术具有无需复杂制样[19-20]、可实现原位在线分析[21-22]及多元素同时检测[23-24]等优点，尤其适用于冶金[25-26]、环境[27-28]、生物化学[29-30]等领域的现场分析。此外，LIBS具有远距离测试的能力，可在高温、辐射等危险环境中替代人工操作、支持生产线实时监控[31]等，因此，远程LIBS受到了更广泛的关注[32]。早在1987年，美国洛斯阿拉莫斯国家实验室Cremers等[33]尝试在 0.5～2.4 m的距离对液态钢中的微量元素进行在线监测。此后，Sun等[34]在冶炼现场对熔融钢液中的Si、Mn、Cr、Ni 和 V 等 5种元素进行定量分析(探测距离为2.8 m)，对比发现偏最小二乘(PLS)模型在相关系数(R^2>0.95)、均方根误差等指标上显著优于单变量定标模型。葛韩星等[35]开展了双脉冲远程LIBS定量装置在20 m探测距离对6种合金钢标样的分析，证实内标法可有效抑制基体效应，提升Cr 和 Mn 等元素的定量精度。

为进一步对比包括内标法在内的不同标准曲线拟合效果差异，本研究基于远程LIBS技术，在最优激光激发次数下采集了12种合金钢标样的光谱。针对钢样中的Cr和Mn，分别利用线性拟合、二次多项式拟合、分段线性拟合及分段内标线性拟合等方式建立定标曲线进行拟合系数对比，得到最佳拟合方式进行定量研究。以预测决定系数(R^2)、相对误差(RE)、相对标准偏差(RSD)、均方根误差(RMSE)等指标评估定量效果，旨在为钢铁工业现场元素快速检测提供定量方案。

1 实验部分

1.1 仪器装置

图1为远程LIBS仪器装置原理图。实验采用Nd:YAG激光器作为激发源，激光波长为1 064 nm，单脉冲能量为20 mJ，重复频率为10 Hz，脉冲宽度为5 ns。脉冲激光通过扩束光路，经施密特-卡塞格林反射式望远镜聚焦至样品表面，对样品激发产生等离子体。等离子体光谱由望远镜收集，经光纤传输至光谱仪(光谱范围为220～645 nm)，通过计算机控制电机驱动望远镜改变次镜位置，从而实现激光聚焦焦点在1～6 m范围内调节。

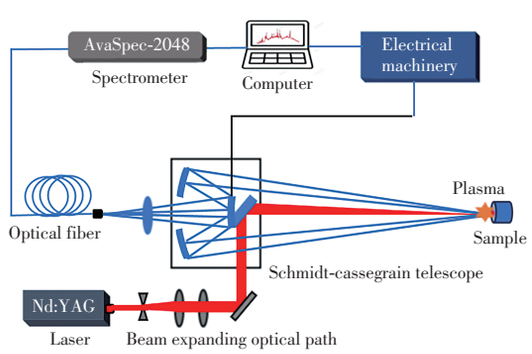


图1 远程 LIBS 实验装置原理示意图

Figure 1 Schematic of the remote LIBS setup.

1.2 样品分析

实验采用12种合金钢标准样品进行测量，样品编号为C01－C12，样品由沈阳市北方标准发行中心研制。钢样中Cr、Mn和Fe含量如表1所示。在相同实验条件下，每个样品累计选取50个不同点位依次进行激光激发和光谱采集，每个点位采集单个光谱，每个样品得到50个光谱数据。为保证测试结果一致性，样品在测试前均进行表面清理。

为定量分析样品中Cr、Mn的预测结果，以相对标准偏差(RSD)、均方根误差(RMSE)、相对误差(RE)、预测决定系数(R^2)等指标评估定量效果，4种指标计算式如下：

表1　钢样中Cr、Mn和Fe含量

Table 1　Content of Cr and Mn in steel samples　/%

Sample number	Standard samples	Mn content	Cr content	Fe content
C01	YSBS 35244-2019	1.61	0.125	97.6
C02	YSBS 35350-2019	0.4	12.45	86.2
C03	YSBS 35476-2019	0.376	5.32	91.4
C04	YSBS 353103-2019	0.56	8.83	89.1
C05	YSBS 352385-2019	0.6	0.92	97.6
C06	YSBS 352012-2020	0.273	1.45	97.0
C07	YSBS 353332-2018	0.325	12.11	85.6
C08	YSBS 41324-2010	0.611	1.02	97.5
C09	YSBS 41118-2014	1.32	0.25	97.5
C10	YSBS281075-2015	0.344	12.1	86.4
C11	YSBS 11265a-2015	1.45	0.079	97.2
C12	ZBG82a	0.838	1.07	97.2

$$\mathrm{RSD}=\frac{1}{\bar{x}}\sqrt{\frac{1}{n-1}\sum_{i=1}^{n}\left(\hat{x}_i-\bar{x}\right)^2}\times 100\% \tag{1}$$

$$\mathrm{RMSE}=\sqrt{\frac{1}{n}\sum_{i=1}^{n}\left(x_i-\hat{x}_i\right)^2} \tag{2}$$

$$\mathrm{RE}=\left|\frac{(x_i-\hat{x}_i)}{x_i}\right|\times 100\% \tag{3}$$

$$R^2=1-\frac{\sum_{i=1}^{s}\left(x_i-\hat{x}_i\right)^2}{\sum_{i=1}^{s}\left(x_i-\bar{x}\right)^2} \tag{4}$$

式中，$\bar{x}$(%)为样品预测值的平均值，n 为测量次数，$\hat{x}_i$(%)是样品的预测值，x_i(%)为样品的标准值，s为样品数量。

2　结果与讨论

2.1　谱线选择与激光累加次数优化

根据原子发射光谱标准数据库中元素谱线分布信息，对光谱仪覆盖范围波长段进行特征谱线提取，按照峰值明显、谱线轮廓无干扰的标准，选定Mn(Ⅰ)403.48 nm和Cr(Ⅰ)520.83 nm作为定量分析谱线，Fe(Ⅰ)438.35 nm作为内标谱线。

为验证该远程LIBS仪器在不同距离的测量效果，选择C02号合金钢样品分别在2、3、4、5 m距离进行光谱采集，Cr(Ⅰ)520.83 nm、Mn(Ⅰ)403.48 nm谱线强度随距离的增加呈下降趋势(图2a、2b)。在2、3 m处可清晰分辨出Cr(Ⅰ)520.83 nm、Mn(Ⅰ)403.48 nm特征峰，而随分析距离增大到5 m时，Mn(Ⅰ)403.48 nm特征峰强度下降明显，这与仪器所用主镜的光学接收效率变化相一致。由于望远镜的收集立体角与距离的平方成反比，随着测量距离增加，望远镜的收集立体角逐渐减小，使主镜能够收集的光子数量减小[36]。为获得更有效的定量方法优化研究，选取3 m的测量距离开展后续定量优化。

选择C02号样品对激光脉冲的激发累加次数进行优化。激光的激发累加次数分别采用1、3、8、13、20、25次，测量距离为3 m。随着激发累加次数的增加，Cr(Ⅰ)520.83 nm、Mn(Ⅰ)403.48 nm谱线强度呈增长趋势(图2c、2d)，但光谱强度提高的同时，光谱韧致辐射所引起的连续背景也会随之提高。因此，需要对不同激发累加次数下的信噪比进行计算。结果显示(图3a)，信噪比(Signal-to-noise Ratio，SNR)随激光激发次数的增加而增加，在激发次数为20次时，两种元素SNR达到最大，其中Cr(Ⅰ)520.83 nm SNR变化显著，这是因为在该激发次数下等离子体激发效率相近，噪声波动较为平稳。进一步对C02号样品采集50次重复光谱进行稳定性验证，结果显示Cr(Ⅰ)520.83 nm、Mn(Ⅰ)403.48 nm谱线强度变化的相对标准偏差分别为6.61%和4.95%(图3b)，说明在20次激光累加下光谱稳定可靠。综上所述，优化后激光的激发累加次数20次时为最佳光谱采集参数。

2.2　定量分析过程及结果

光谱在采集过程中易受环境变化、仪器噪声和基质效应等因素的影响，导致每次采集的光谱会形成基线漂移或基线倾斜的现象，对实验的定量准确度造成影响。基线校正能够分离光谱信号和背景噪声，得到光谱净信号。本研究采用自适应加权最小二乘法(Asymmetric Least Squares，ALS)实现光谱基线校正，该方法通过构建含光谱数据拟合项与平滑惩罚项的目标函数，进行不对称权重迭代优化，实现基线拟合并扣除基线。图4为该方法在Cr(Ⅰ)520.83 nm、Mn(Ⅰ)403.48 nm谱线附近波段去基线与未去基线的对比图，分离基线后光谱无基线漂移及基线倾斜现象，且未改变谱线形状。平滑可以减少光谱信号中高频随机噪声，使谱峰轮廓更清晰。归一化是指将整条光谱的强度值按一定比例缩放，使不同样品获得的光谱具有可比性。为研究不同预处理对数据的影响，对C02号样品所有光谱数据进行基线校正、平滑及0～1归一化三种预处理，只经基线校正处理Cr(Ⅰ)520.83 nm峰强度的RSD值为6.85%，经基线校正结合平滑处理Cr(Ⅰ)520.83 nm峰强度的RSD值为6.99%，经基线校正、平滑及0～1归一化处理Cr(Ⅰ)

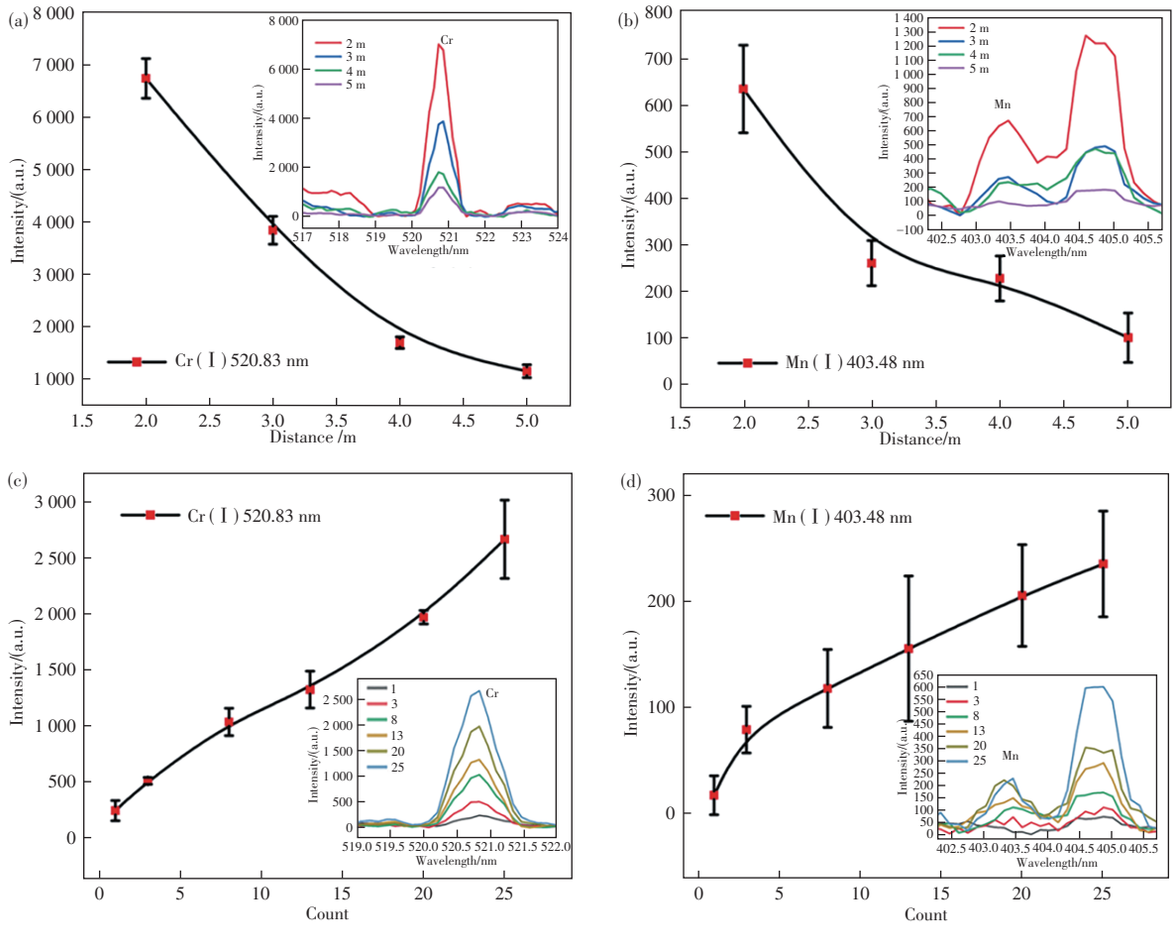


图2　Cr与Mn条件优化图：(a)、(b)不同距离的光谱图；(c)、(d)不同激发累加次数的光谱图

Figure 2　Condition optimization diagrams of Cr and Mn: (a), (b) Spectra at different distances; (c), (d) Spectra with different excitation accumulation times.

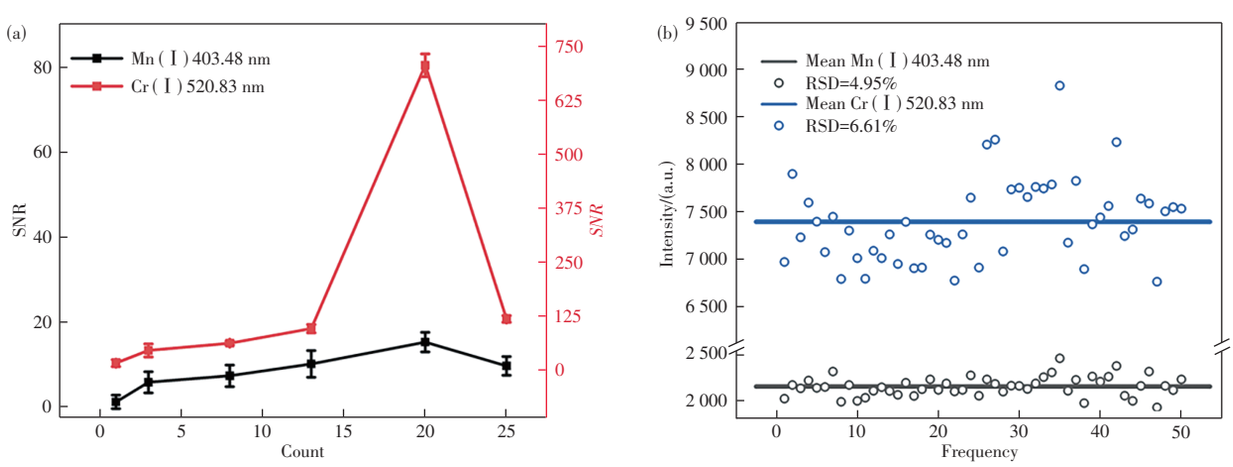


图3　Cr与Mn信噪比及相对标准偏差：(a)不同激发累加次数信噪比图；(b)Cr、Mn 50次光谱采集的相对标准偏差

Figure 3　Signal-to-noise ratio and relative standard deviation plots for Cr and Mn: (a) SNR diagram with different excitation accumulation times; (b) RSD of 50 spectra acquisitions for Cr and Mn.

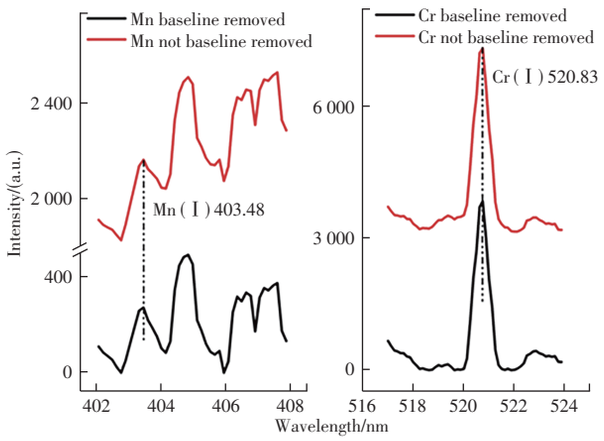


图4　Cr、Mn去基线与未去基线的对比图

Figure 4　Comparison of Cr and Mn with and without baseline removal.

520.83 nm峰强度的RSD值为0.04%。而原始数据Cr(Ⅰ)520.83 nm峰强度的RSD值为6.16%，说明三种预处理方式通过消除数据量纲差异、减少量纲不一致导致的误差，使数据稳定，而基线校正和平滑处理为归一化处理提供了较好的数据基础。因此，将所有光谱数据均进行基线校正、平滑及0～1归一化处理。

为对比不同拟合方法标定曲线的拟合系数，选择样品C04、C07作为验证样品，其余样品作为标准样品，利用线性拟合、二次多项式拟合、分段线性拟合及分段内标线性拟合方式分别建立Cr、Mn的定标曲线。其中分段方式标准曲线分段点的优化过程是将各样品按强度值从小到大排列，然后从第3到第7个点依次分为两段，计算两段预测值的总残差平方和，当总残差平方和最小时认为对应分段点为最优，优化后Cr的分段点均为6，Mn线性分段点为7、内标线性分段点为6。各拟合方式Cr、Mn的定标曲线如图5、6所示。对比Cr标准曲线，由于激光与物质相互作用产生的等离子体信号受到许多复杂因素的干扰，例如激光能量在远距离传输损耗导致到达样品表面的激光辐照度减小进而影响等离子体产生[37]、大气中的气体分子使传输过程的等离子体信号发生波动等[38]，使得不同含量Cr的光谱强度在不同区间产生局部变化。分段内标线性拟合方式通过划分两个区间使不同区间线性拟合更适应光谱的变化，又因为引入了内标元素，有效降低了基质差异的影响，

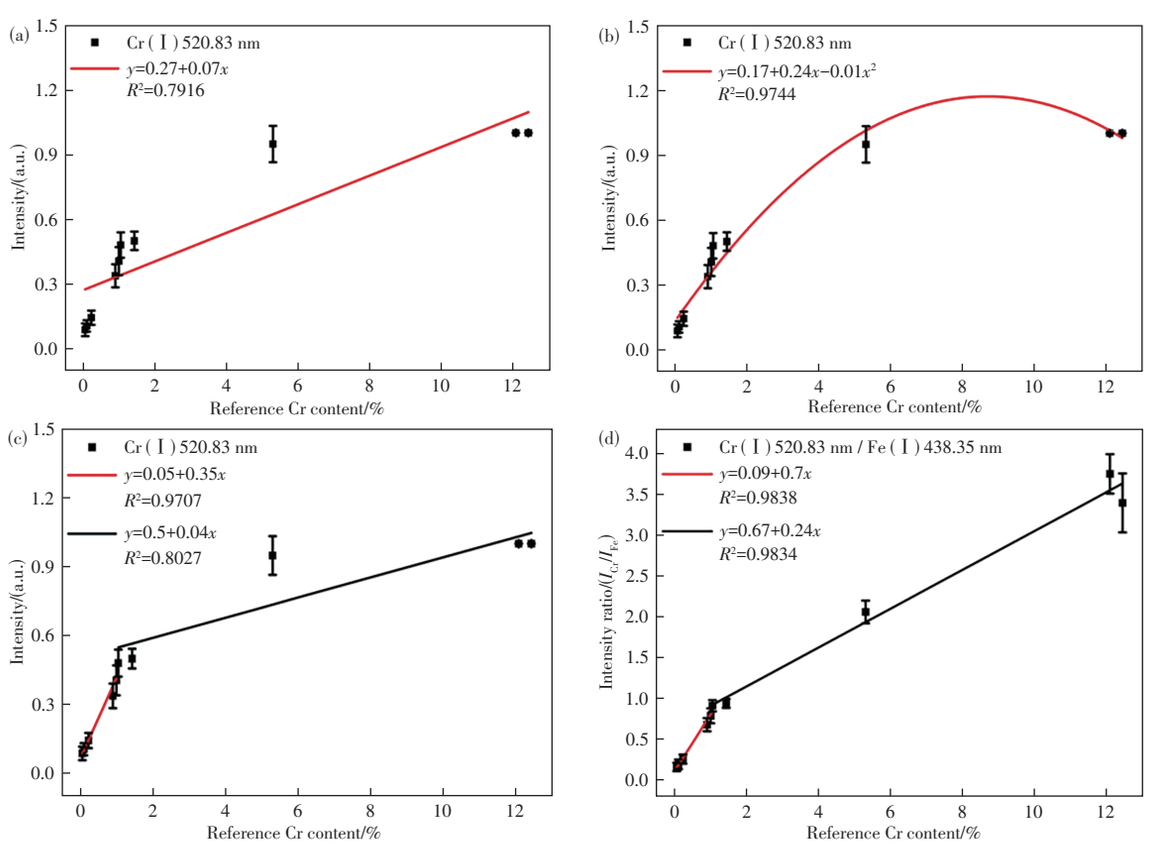


图5　不同拟合方法下Cr的定标曲线：(a)线性拟合标曲；(b)二次多项式拟合标曲；(c)分段线性拟合标曲；(d)分段内标线性拟合标曲

Figure 5　Calibration curves of Cr with different fitting methods: (a) Linear; (b) Quadratic; (c) Piecewise linear; (d) Piecewise internal standard linear fit.

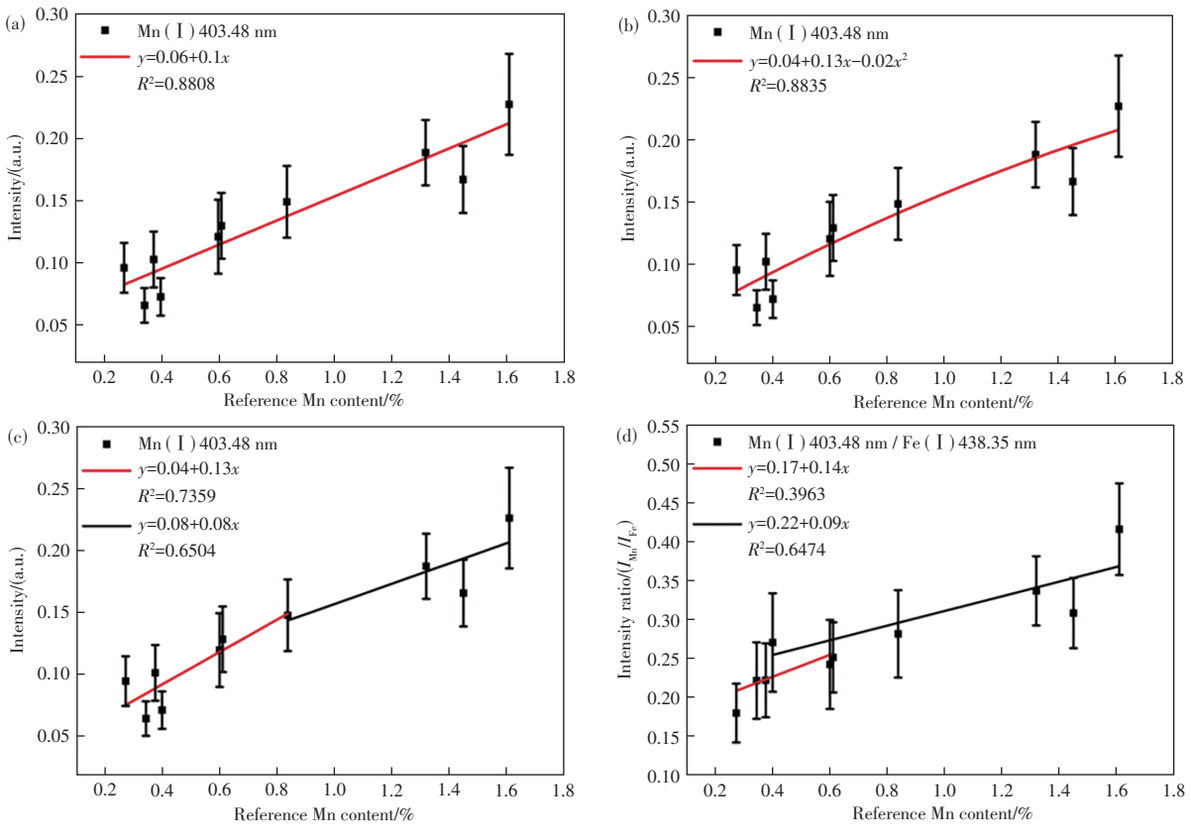


图6 不同拟合方式下Mn的定标曲线：(a)线性拟合标曲；(b)二次多项式拟合标曲；(c)分段线性拟合标曲；(d)分段内标线性拟合标曲

Figure 6 Calibration curves of Mn with different fitting methods: (a) Linear; (b) Quadratic; (c) Piecewise linear; (d) Piecewise internal standard linear fit.

从而显著提高了定标曲线的拟合度，其两段线性标准曲线(简称“标曲”)R^2数值均高于0.98，且各标样点更接近拟合曲线。Mn则以二次多项式拟合效果最优，R^2值为0.883 5，其余三种拟合方式数据点较为分散。为探究分段内标线性拟合方式对Cr在不同距离拟合度提升的普适性，分别在2、4和5 m距离对标准样品进行相同光谱采集，采用相同预处理方式处理后对Cr建立4种拟合方式的标定曲线。结果显示，在2 m距离分段内标线性拟合方式效果最优，两段线性标定曲线拟合度均优于0.998，而在4和5 m距离均为二次多项式拟合效果最优。因此，在3 m距离范围内分段内标线性拟合方式能有效提高定标曲线的拟合度。综上所述，分别选择分段内标线性拟合方式对Cr采用分段内标线性拟合、对Mn采用二次多项式拟合进行后续定量。

表2为验证样品中Cr、Mn的定量结果。对比标准值与预测值的结果，C04号样品Cr、Mn预测值的相对误差分别为14.4%、9.82%，均方根误差分别为1.40%、0.090%，C07号样品Cr、Mn预测值的相对误差分别为8.34%、7.38%，均方根误差分别为1.09%、0.049%。为探究预测值的重复性，需进行相对标准偏差的计算，由表2可得C04号样品Cr、Mn预测值的相对标准偏差分别为3.7%、12.7%，C07号样品Cr、Mn预测值的相对标准偏差分别为6.8%、11.3%。定量结果显示通过对定标曲线的优化选择，有助于提高远程LIBS技术定量结果的准确度与精密度。

表2 Cr和Mn的定量结果

Table 2 Quantitative results of Cr and Mn /%

Items	Cr		Mn	
	Segmented internal standard linear fitting		Quadratic polynomial fitting	
Sample number	C04	C07	C04	C07
Standard content	8.83	12.11	0.56	0.325
Predicted content	10.1	11.1	0.505	0.301
Relative error	14.4	8.34	9.82	7.38
Root mean square error	1.40	1.09	0.090	0.049
Relative standard deviation	3.7	6.8	12.7	11.3

3　结论

基于远程LIBS仪器对合金钢中的Cr、Mn两种元素进行了定量分析，验证了该仪器对钢铁中元素定量的可行性。分析最优参数及最佳拟合方式定量结果，远程LIBS仪器对合金钢中的Cr、Mn两种元素预测值的相对误差最小值分别为8.34%和7.38%，均方根误差最小值分别为1.09%和0.049%，相对标准偏差最小值分别为3.7%和11.3%。研究结果显示，利用单变量定标方法通过优化分析参数及拟合方式进行定量，可为合金钢中元素的工业现场检测提供一种简单可靠的定量方案。

参考文献

[1] 王云雾. 基于低碳减排要求下的钢铁冶金绿色技术应用探讨[J]. 山西冶金，2023，46(12)：67-69.
Wang Yunji. Discussion on the application of green technologies in steel metallurgy based on low-carbon emission reduction requirements[J]. Shanxi Metallurgy, 2023, 46(12): 67-69.

[2] 魏宽. 远程激光诱导击穿光谱技术研究[D]. 西安：西安电子科技大学，2023.
Wei Kuan. Study on remote laser-induced breakdown spectroscopy technology[D]. Xi'an: Xidian University, 2023.

[3] Sun Jianlin, Tang Huajie, Wang Chenglong, et al. Effects of alloying elements and microstructure on stainless steel corrosion: a review[J]. Steel Research International, 2022, 93(5): 2100450. DOI: 10.1002/srin.202100450.

[4] 余宗森，袁泽喜，李定秀，等. 鞍钢钢材成分与其力学性能的定量关系[J]. 北京科技大学学报，1997，19(5)：510-515.
Yu Zongsen, Yuan Zexi, Li Dingxiu, et al. Quantitative relationship between mechanical properties and chemocal compositions of steels made by Anshan iron and steel corporation[J]. Journal of University of Science and Technology Beijing, 1997, 19(5): 510-515.

[5] Cardoso A S M, Pardal J M, Souza A P, et al. Thermal aging effects on mechanical and intergranular corrosion resistance of super-austenitic stainless steel exposed at 600 ℃ [J]. Materials Research, 2022, 25(S1): e20220079. DOI: 10.1590/1980-5373-mr-2022-0079.

[6] Ajeel S A. Green corrosion inhibitor for protection of mild steel[J]. Engineering and Technology Journal, 2017, 35(9): 914-921.

[7] Zhang Yong, Jia Yunhai, Chen Jiwen, et al. Comparison of the analytical performances of laser-induced breakdown spectroscopy and spark-OES[J]. ISIJ International, 2014, 54(1): 136-140.

[8] Hemmerlin M, Meilland R, Falk H, et al. Application of vacuum ultraviolet laser-induced breakdown spectrometry for steel analysis: comparison with spark-optical emission spectrometry figures of merit[J]. Spectrochimica Acta Part B: Atomic Spectroscopy, 2001, 56(6): 661-669.

[9] Xu Shukun, Sun Lijing, Fang Zhaolun. Determination of gold in ore by flame atomic absorption spectrometry with flow-injection on-line sorbent extraction preconcentration[J]. Analytica Chimica Acta, 1991, 245: 7-11.

[10] Chilian A. Introduction of curvature index and improvement of calibration curves used in ion chromatography (IC), atomic absorption spectrometry (AAS), UV-Vis spectrophotometry and catalytic combustion[J]. Analytica Chimica Acta, 2025, 1336: 343521. DOI: 10.1016/j.aca.2024.343521.

[11] Thangavel S, Dash K, Dhavile S M, et al. Determination of traces of As, B, Bi, Ga, Ge, P, Pb, Sb, Se, Si and Te in high-purity nickel using inductively coupled plasma-optical emission spectrometry (ICP-OES)[J]. Talanta, 2015, 131: 505-509.

[12] Poimenova I A, Zhukova E Y, Ovseenko S T, et al. Detailed impurity profiling of graphene oxide fractions by robust inductively coupled plasma optical emission spectrometry monitoring[J]. Analytica Chimica Acta, 2026, 1392: 345140. DOI: 10.1016/j.aca.2026.345140.

[13] Tavares T R, Demattê J A M, Bedum G V, et al. Rapid in situ analysis with portable XRF sensor: a pioneering study proposing fitness-for-purpose approach for performance assessment in tropical soils[J]. Soil Security, 2026, 22: 100228. DOI: 10.1016/j.soisec.2026.100228.

[14] Li Zelan, Scagliarini C, Mazzoleni A, et al. Exploiting the penetration depth of XRF and NIR radiation: from 2D to 3D spectral imaging[J]. TrAC Trends in Analytical Chemistry, 2026, 197: 118693. DOI: 10.1016/j.trac.2026.118693.

[15] Wüstkamp D, Kucharkowski R, Broekaert J A C. Highly accurate analysis of soft magnetic alloys by automated sample digestion and simultaneous ICP-OES[J]. Fresenius' Journal of Analytical Chemistry, 1996, 355(3): 281-283.

[16] Mzyk Z, Anyszkiewicz J, Matusiak H. Analysis of alloy composition by X-ray fluorescence spectrometry using liquid and thin layer techniques with an internal standard[J]. Spectrochimica Acta Part B: Atomic Spectroscopy, 2012, 69: 44-49.

[17] Zhao Wenya, Li Chen, Yan Chenglin, et al. Interpretable deep learning-assisted laser-induced breakdown spectroscopy for brand classification of iron ores[J]. Analytica Chimica Acta, 2021, 1166: 338574. DOI: 10.1016/j.aca.2021.338574.

[18] Li Fang, Lu Anxiang, Wang Jihua. Modeling of chromium, copper, zinc, arsenic and lead using portable X-ray fluorescence spectrometer based on discrete wavelet transform[J]. International Journal of Environmental Research and Public Health, 2017, 14(10): 1163. DOI: 10.3390/ijerph14101163.

[19] 舒开强, 许应铜, 高智星, 等. 激光诱导击穿光谱对U的定量分析[J]. 中国无机分析化学, 2024, 14(2): 139-144.
Shu Kaiqiang, Xu Yingtong, Gao Zhixing, et al. Quantitative analysis of U by laser-induced breakdown spectroscopy[J]. Chinese Journal of Inorganic Analytical Chemistry, 2024, 14(2): 139-144.

[20] Liu Xiaona, Zhang Qiao, Wu Zhisheng, et al. Rapid elemental analysis and provenance study of Blumea balsamifera DC using laser-induced breakdown spectroscopy[J]. Sensors, 2014, 15(1): 642-655.

[21] 廖文龙, 刘坤平, 胡建平, 等. 指纹光谱病原菌快速检测研究进展与趋势[J]. 光谱学与光谱分析, 2021, 41(8): 2372-2377.
Liao Wenlong, Liu Kunping, Hu Jianping, et al. Research advances and trends of rapid detection technologies for pathogenic bacteria based on fingerprint spectroscopy[J]. Spectroscopy and Spectral Analysis, 2021, 41(8): 2372-2377.

[22] Gaft M, Nagli L, Groisman Y, et al. Industrial online raw materials analyzer based on laser-induced breakdown spectroscopy[J]. Applied Spectroscopy, 2014, 68(9): 1004-1015.

[23] 舒开强, 陈友元, 彭郑英, 等. 铀矿中多目标元素的激光诱导击穿光谱定量分析方法研究[J]. 分析化学, 2023, 51(7): 1195-1203.
Shu Kaiqiang, Chen Youyuan, Peng Zhengying, et al. Laser-induced breakdown spectroscopy for quantitative analysis of multi-target elements in uranium ore[J]. Chinese Journal of Analytical Chemistry, 2023, 51(7): 1195-1203.

[24] Lednev V N, Sdvizhenskii P A, Grishin M Y, et al. Laser induced breakdown spectroscopy for multielement analysis of powdered materials used in additive technologies[J]. Spectroscopy Letters, 2018, 51(4): 184-190.

[25] 牛广辉, 张业建, 林庆宇. 激光诱导击穿光谱(LIBS)技术在低碳钢铁冶金行业的应用[J]. 中国无机分析化学, 2024, 14(2): 168-175.
Niu Guanghui, Zhang Yejian, Lin Qingyu. Application of laser-induced breakdown spectroscopy in low-carbon steel metallurgy industry[J]. Chinese Journal of Inorganic Analytical Chemistry, 2024, 14(2): 168-175.

[26] Pedarnig J D, Trautner S, Grünberger S, et al. Review of element analysis of industrial materials by In-line laser-induced breakdown spectroscopy (LIBS)[J]. Applied Sciences, 2021, 11(19): 9274. DOI: 10.3390/app11199274.

[27] Harmon R S, Russo R E, Hark R R. Applications of laser-induced breakdown spectroscopy for geochemical and environmental analysis: a comprehensive review[J]. Spectrochimica Acta Part B: Atomic Spectroscopy, 2013, 87: 11-26.

[28] Gaudiuso R, Dell′Aglio M, De Pascale O, et al. Laser induced breakdown spectroscopy for elemental analysis in environmental, cultural heritage and space applications: a review of methods and results[J]. Sensors, 2010, 10(8): 7434-7468.

[29] 任文心, 杨亮, 赵韩, 等. 激光诱导击穿光谱定量分析全血中的锂元素[J]. 分析化学, 2024, 52(4): 559-565.
Ren Wenxin, Yang Liang, Zhao Han, et al. Quantitative analysis of lithium element in whole blood using laser-induced breakdown spectroscopy[J]. Chinese Journal of Analytical Chemistry, 2024, 52(4): 559-565.

[30] Bhatt C R, Jain J C, Goueguel C L, et al. Determination of rare earth elements in geological samples using laser-induced breakdown spectroscopy (LIBS)[J]. Applied Spectroscopy, 2018, 72(1): 114-121.

[31] Zhang Zhezhe, Deguchi Y, Shiou F, et al. Feasibility investigation for online elemental monitoring of iron and steel manufacturing processes using laser-induced breakdown spectroscopy[J]. ISIJ International, 2020, 60(5): 971-978.

[32] 宋骁冉, 牛广辉, 汤悦, 等. 小型化远程激光诱导击穿光谱仪器研发及对合金钢中硅钼铬的分析[J]. 冶金分析, 2024, 44(9): 8-13.
Song Xiaoran, Niu Guanghui, Tang Yue, et al. Development of miniaturized remote laser-induced breakdown spectroscopy instrument and its application in analysis of silicon, molybdenum and chromium in alloy steel[J]. Metallurgical Analysis, 2024, 44(9): 8-13.

[33] Cremers D A. The analysis of metals at a distance using laser-induced breakdown spectroscopy[J]. Applied Spectroscopy, 1987, 41(4): 572-579.

[34] Sun Lanxiang, Yu Haibin, Cong Zhibo, et al. In situ analysis of steel melt by double-pulse laser-induced breakdown spectroscopy with a Cassegrain telescope[J]. Spectrochimica Acta Part B: Atomic Spectroscopy, 2015, 112: 40-48.

[35] 葛韩星，魏宽，侯佳佳，等. 合金钢中微量元素的双脉冲激光诱导击穿光谱远程定量分析[J]. 冶金分析，2023，43(8)：10-16.
Ge Hanxing，Wei Kuan，Hou Jiajia，et al. Remote quantitative analysis of trace element in alloy steels by dual-pulse laser-induced breakdown spectroscopy[J]. Metallurgical Analysis，2023，43(8)：10-16.

[36] 曹溪源，骆益凡，赵阳阳，等. 远程激光诱导击穿光谱金属定性定量分析研究[J]. 中国激光，2025，52(6)：311-321.
Cao Xiyuan，Luo Yifan，Zhao Yangyang，et al. Qualitative and quantitative analysis of metals via remote laser induced breakdown spectroscopy[J]. Chinese Journal of Lasers，2025，52(6)：311-321.

[37] 刘瑞斌，殷允嵩. 激光诱导击穿光谱技术相关物理机制研究进展[J]. 中国光学(中英文)，2024，17(1)：19-37.
Liu Ruibin，Yin Yunsong. Research progress on the related physical mechanism of laser-induced breakdown spectroscopy[J]. Chinese Optics，2024，17(1)：19-37.

[38] 何亚雄，周文琦，柯川，等. 激光诱导击穿光谱技术在气体检测中的研究综述[J]. 光谱学与光谱分析，2021，41(9)：2681-2687.
He Yaxiong，Zhou Wenqi，Ke Chuan，et al. Review of laser-induced breakdown spectroscopy in gas detection[J]. Spectroscopy and Spectral Analysis，2021，41(9)：2681-2687.

Quantitative Analysis of Chromium and Manganese in Alloy Steel by Remote Laser-induced Breakdown Spectroscopy(LIBS)

Chen Xi[1,2], Li Yuanke[3], Yue Hongcheng[3], Tang Yue[3], Tian Junlang[1,2], Niu Guanghui[4*], Sun Xuan[1,2*], Lin Qingyu[3*]

(*1. Key Laboratory of Advanced Manufacturing and Automation Technology, Guilin University of Technology, Guilin, Guangxi 541006, China;*
2. College of Mechanical and Control Engineering, Guilin University of Technology, Guilin, Guangxi 541004, China;
3. School of Mechanical Engineering, Sichuan University, Chengdu, Sichuan 610064, China;
4. Baowu Equipment Intelligent Technology Co., Ltd., Research and Development Center, Shanghai 201900, China)

Abstract The detection of chemical element compositions in steel products or raw materials is a critical factor in ensuring product quality control. Laser-induced breakdown spectroscopy (LIBS) technology, distinguished by its capability for remote testing, enables in situ quantitative analysis of production items from a distance, even in hazardous environments characterized by high temperatures and radiation. In this study, leveraging a portable remote LIBS instrument, spectral data were collected from 12 alloy steel standard samples at a 3 m distance after optimizing the cumulative excitation count of laser pulses. The collected data underwent three preprocessing methods: baseline correction alone, baseline correction with smoothing, and baseline correction with smoothing and 0—1 normalization. A comparative analysis revealed that the preprocessing method involving baseline correction, smoothing, and 0—1 normalization yielded the best data processing results, reducing the relative standard deviation (RSD) from 6.16% to 0.04%. Notably, normalization played a dominant role in improving the RSD. Consequently, all spectral data were subjected to baseline correction, smoothing, and 0—1 normalization. Subsequently, calibration curves were established using linear fitting, quadratic polynomial fitting, piecewise linear fitting with optimized segment points, and piecewise internal standard linear fitting. A comparative assessment of these four fitting methods demonstrated that the piecewise internal standard linear fitting method was optimal for Cr(Ⅰ) at 520.83 nm, with R^2 values exceeding 0.98 for both segments of the linear calibration curve. For Mn(Ⅰ) at 403.48 nm, the quadratic polynomial fitting method exhibited the best fitting performance, with an R^2 value of 0.883 5. Based on the fitting methods with the highest degree of fit, piecewise internal standard linear fitting was selected for the quantitative analysis of Cr, and quadratic polynomial fitting was chosen for Mn. Quantitative analysis results from two validation samples showed that the minimum relative errors of the predicted values for Cr and Mn were 8.34% and 7.38%, respectively, with maximum values of 14.4% and 9.82%. The minimum root mean square errors were 1.09% and 0.049%, with maximum values of 1.40% and 0.090%. The minimum relative standard deviations were 3.7% and 11.3%, with maximum values of 6.85% and 12.7%. These findings

substantiate the feasibility of using this instrument for quantitative analysis of steel elements. This study confirms that employing a univariate calibration approach, by optimizing analytical parameters and fitting methods, provides a straightforward and reliable quantitative solution for on-site industrial detection of elements in alloy steels, thereby offering a valuable tool for quality control in the steel manufacturing industry. This study confirms that employing a univariate calibration approach, by optimizing analytical parameters and fitting methods, provides a straightforward and reliable quantitative solution for on-site industrial detection of elements in alloy steels, thereby offering a valuable tool for quality control in the steel manufacturing industry.

Keywords laser-induced breakdown spectroscopy; remote quantitative analysis; alloy steel; Cr; Mn

HIGHLIGHTS

1) Quantitative analysis of Cr and Mn elements in alloy steel standard samples was performed using a remote LIBS system.
2) The influence of different laser excitation frequencies on characteristic spectra was optimized.
3) The effects of four calibration curve fitting methods were investigated, and the segmentation points for piecewise fitting were optimized.